SUPPLEMENTARY MATERIALS

THE PHYSICAL MODEL

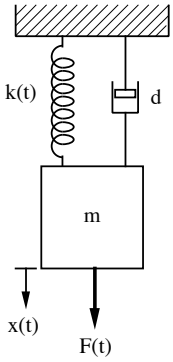

Figure 1. A simplified model of the physical system, depicting a single normal mode

The aim is to determine the force $F(t)$ from a measurement of $x(t)$ using a resonant capacitive transducer. The spring constant is modulated by the voltage $V_B(t)$ applied to the capacitive transducer

$$k(t) = k_0 - a\,V_B^2(t) \tag{1}$$

where k_0 is the natural spring constant and a describes the strength of the transducer coupling to the modulation process. The modulation is produced by a square wave at about 3 Hz, which is passed through a low pass filter before amplification to high voltage and the amplified signal is applied to the transducer. The frequency response of the amplifier coupled to the capacitive is unknown and must be determined either experimentally or by modelling the amplifier. It is possible that the damping is also modulated, but this cannot be confirmed until some preliminary processing has been completed.

The displacement $x(t)$ is sensed by a resonant capacitive transducer and demodulated to produce the measured signal $V_x(t)$. The demodulation produces an unknown delay, which must be determined either experimentally or by modelling the transducer and demodulation system.
The differential equation is

$$m\frac{d^2}{dt^2}x(t) = F(t) - k(t)\,x(t) - d\frac{d}{dt}x(t) \tag{2}$$

and this is non-linear, requiring a numerical solution.

The force $F(t)$ is slowly varying and can be assumed constant during each period of the bias voltage.

THE DATA

Fig. 2 shows an extract of the acquired data under stationary condition before the field trial commenced. The grey trace represents the input to the HV amplifier, and the red trace represents the demodulated data. The reason for the apparent delay is unknown but the delay must be included in the model.

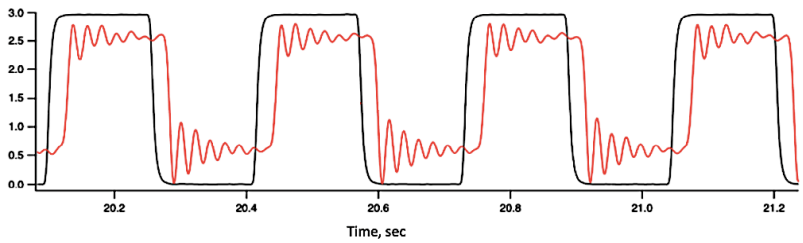

Figure 2. Extract from the pre-field-test data recoded under stationary conditions

THE MODEL

The output signal $V(t)$ is assumed to be proportional to the displacement delayed by a fixed latency Δt

$$V(t) = \sigma\, x(t - \Delta t) \tag{3}$$

This assumes that the latency is due to the demodulation electronics and not the modulation of the stiffness. Equation 2 can be recast in the form

$$\frac{d^2}{dt^2}x(t) = A(t) - f_o^2\left(1 - \alpha\, V_B^2(t)\right) x(t) - \beta \frac{d}{dt}x(t) \tag{4}$$

Defining $\mathrm{y(t)} = \frac{d}{dt}\mathrm{x(t)}$,, this gives two coupled first order differential equations

$$\begin{aligned} y(t) &= \tfrac{d}{dt}x(t) \\ \tfrac{d}{dt}y(t) &= A(t) - f_o^2\left(1 - \alpha\, V_B^2(t)\right) x(t) - \beta\, y(t) \end{aligned} \tag{5}$$

Equation 5 contains several free parameters, including α and β, which are simple scalars and A(t), which can be describes in terms of a list of discrete values

$$A_i = A\left(mod\left(t_j, T\right)\right)$$

where T is a characteristic time interval, during which A remains constant, and can be taken to be an integer multiple of the period of the modulating square wave. The index j represents the discrete samples of the continuous signal in equation 5, such that

$$t_j = j\delta t,\ x_j = x\left(t_j\right), y_j = y\left(t_j\right)$$

$$and\ V_{B,j} = V_B\left(t_j\right),$$

where δt is the interval between samples.

The differential equation 5 can be solved if the parameters f_o, α, β and A_i are known and the predicted output signal can then be obtained from equation 3, which introduces two initial parameters Δ and σ. This predicted signal can be compared with the measured output signal and the parameters can then be adjusted using a least-squares algorithm to make the predicted signal match the observed signal. This procedure is computationally expensive, as the full non-linear differential equation must be solved for each iteration of the fit. The parameter σ cannot be obtained independently from the data and must be determined by calibration. The rapid change in equilibrium position of the mass due to the rapid change in $k(t)$ excites the resonance, which rings down with a time constant longer than the half-period of the square wave, the processing is required to extract the equilibrium position from this ringdown.

THE SIMPLIFIED MODEL

Figure 2 indicates that the frequency of the resonant mode, which is excited by the modulation is the same for the rising edge and the falling edge, which is inconsistent with the equation 1, which predicts that the fundamental frequency for the two cases is different. In practice, there are numerous resonant modes in the system and perhaps the fundamental mode predicted by k and m is not the dominant one. Indeed, Fig. 1 depicts a lumped system, whereas in practice it is distributed, giving rise to more modes than the system depicted there, not all of which are modulated by the capacitive transducer. Therefore, it might be unnecessary to solve equation 5 for the two resonant frequencies corresponding to the two modulation states, and the observed resonant frequency can be obtained from the data, which is sufficient to determine the equilibrium position, by performing a curve fit to the ringdown, assuming that

$$x(t) = A\, e^{t/\tau}\ sin(2\pi f_o t + \varphi) \tag{6}$$

with A, $\mathrm{f_o}$, τ and φ determined from the data for each step.

The change in the value of A before and after each step depends on two factors. The first is the value of the external force being applied (ideally through the gravity gradient) and the second is forces applied by the

modulation capacitor, due to imperfect geometry. Ideally, the force exerted by the capacitor on the ribbon is zero but there will be a small residual force due to the geometrical imperfections. However, this is unimportant provided that this force remains constant for each step. The algorithm for extracting the equilibrium positions is described in the next section.

THE PROCESSING ALGORITHM

The data may contain many steps and the main requirement is to identify these steps and process each one individually. An example data set is shown in figure 3.

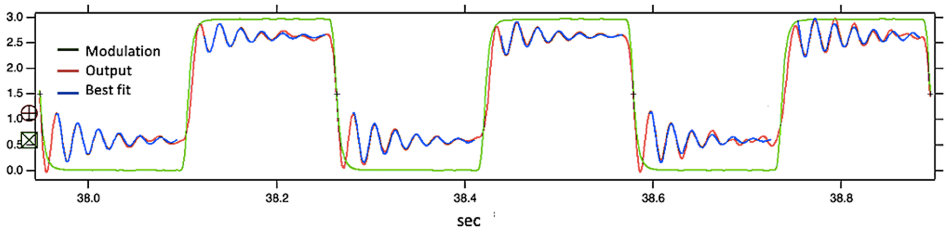

Figure 3. An extract from the processing record

In this figure, the modulation and output signals have been synchronised. This permits easy identification of the corresponding step in the output data. For each step, the equilibrium position is found using a least square fit to a subset of the response data. The first period of the ring-down is ignored, because it is affected by the smoothing of the modulation signal. The non-linear least-squares fit to a sinusoid is not straight forward because if the starting values of the parameters are not sufficiently close to the correct ones, then the fit may not converge and return incorrect parameters.

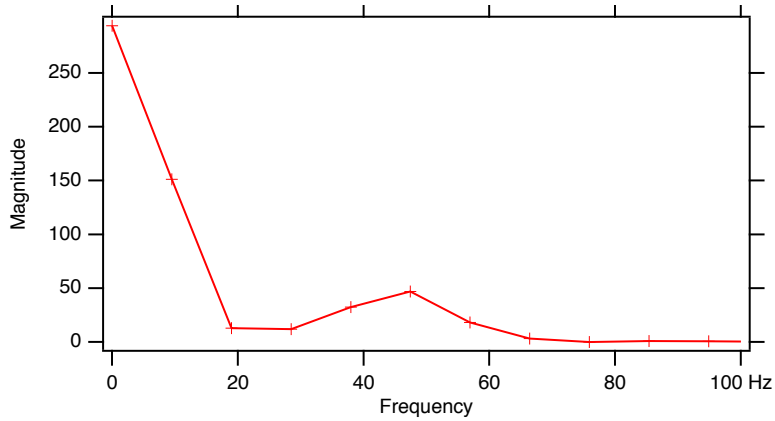

Figure 4. A typical Fourier transform

A Fourier transform of the subset of data is used to obtain the first estimate of the parameters and the magnitude of a typical transform of one of the steps is shown in Fig. 4, indicating a resonance at about 45 Hz. However, because the record is short, containing only a few cycles, the estimated frequency might not be sufficiently close for reliable curve fitting. Therefore, a simplified fit is performed, which ignores the ringdown and uses a simple sinusoid to obtain a better estimate of the frequency.

Finally, a full fit is performed to obtain all four parameters in equation 6 and this converged successfully for each of the 300 steps in the data record, and these parameters are stored as a time sequence. The desired parameter is the equilibrium position following each step and the corresponding sequences for these are shown in Fig. 5. The green crosses show the position corresponding to the off state of the modulation, while the blue crosses show that for the on state. The corresponding size of the step is shown as the red curve and should be proportional to the applied force.

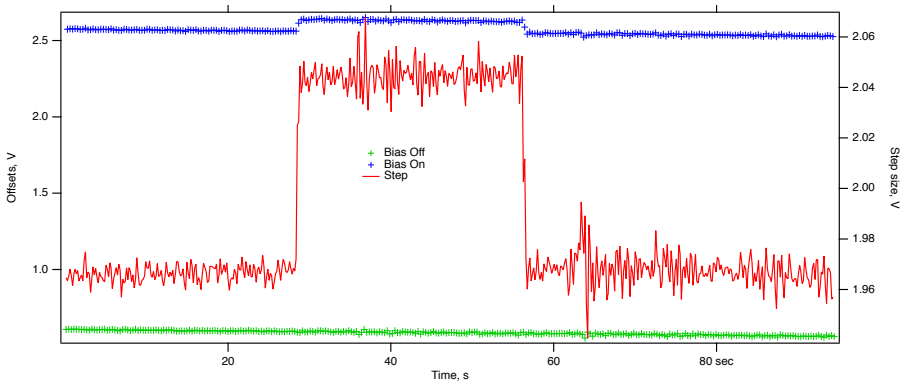

Figure 5. The equilibrium position following each step.

A massive object (a medium size car) was brought to within about 3 m of the sensor at t = 28 s and subsequently removed at t = 57 s, and this produced the change observed in the red line. The frequencies obtained do not correspond to any of the known mechanical modes of the ribbon. The Fourier transform of the entire data set is shown in Fig. 6

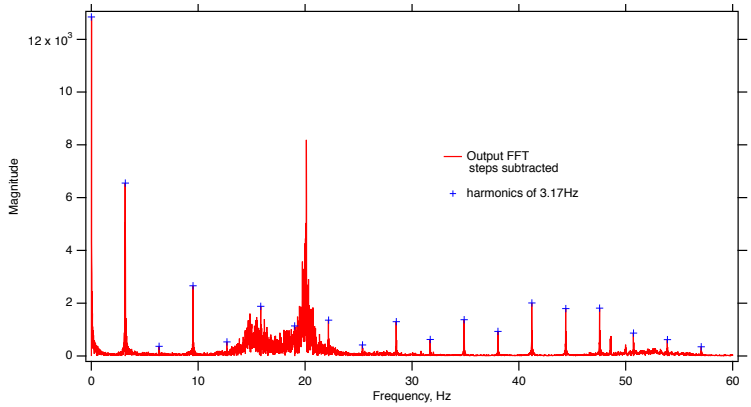

Figure 6. Fourier transform of the data set

The fundamental frequency of the modulation has been suppressed to enhance the dynamic range of the graph but the fundamental and its harmonics, which are depicted by the blue crosses are quite evident. The 45 Hz signal found from the fitting is however not evident, because it is not phase coherent over the entire data set.

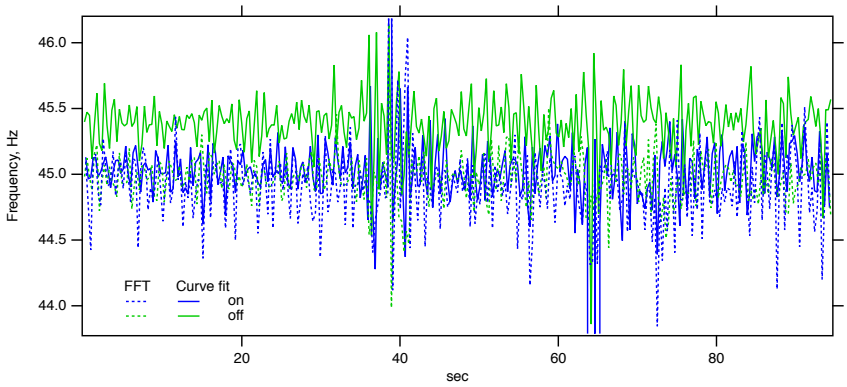

Figure 7. Time series of the frequencies obtained from the fitThe dashed lines show the corresponding frequencies obtained from the Fourier transform, and while these two different measurements are in agreement for the on state, there is a systematic difference for the off state, which is not explained.

The frequencies obtained by fitting are plotted as a time sequence in Fig. 7, where the colour coding is similar to that in Fig. 5. The solid lines show the results of the fit, with green representing the modulation on the off state and blue the on state.

Another view of this is shown in figure 8.

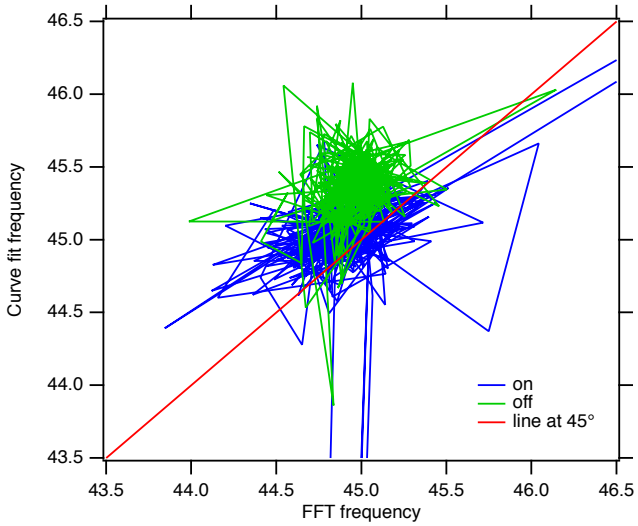

Figure 8. Parametric plot of the frequencies measured by the curve fit and Fourier transform.

If the two methods for obtaining the frequencies are in agreement, the "blobs" would be centred along the red line, plotted at 45°. The reason for this discrepancy is not understood. It might be related to the coarse quantisation of the frequency axis of the Fourier transform, although the position of the peak is obtained by fitting rather than simply taking the frequency at which the peak value occurs.

There are some evident outliers in the frequency plots, a few of which extend beyond the range of the graph. A tool was created to visually examine each step in detail to determine whether the results seem reliable. The two controls at the top of the graph make this convenient, because they permit the graph to be zoomed in to any individual step or optionally some number of consecutive steps. The variable N determines the index of the first step shown and ΔN determines the number of steps shown. A few typical outliers are shown in Fig. 9. The reason for this behavior is not explained, but it is clear that for these steps, a different mixture of the normal modes was excited.

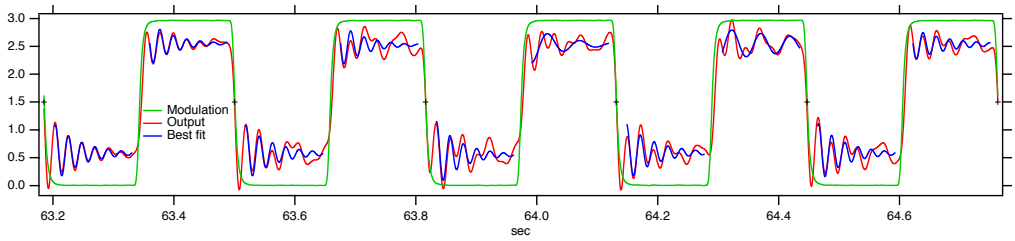

Figure 9. A few outliers

THE FIELD DATA

The field data shows much greater excitation of the mechanical modes. Many modes are excited simultaneously, making it meaningless to fit a single decaying sinusoid. In these circumstances, the most reliable method of determining the equilibrium position is to perform a simple average instead of a fit as depicted in Fig. 10 below.

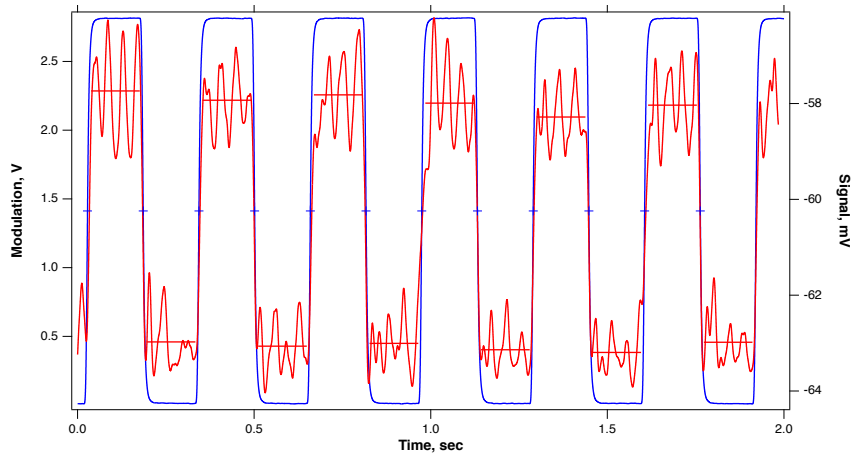

Figure 10. The modulation signal (blue) and output signal (red)

In all cases the field data consists of a large number of individual data files (in .csv format), one for each station and a special signal processing GUI, based on either professional Igor Pro 9 or MatLab software environment, were developed to view the all together in the same graph. The inclinometer data were included in the processing algorithm as shown in Fig. 11 below.

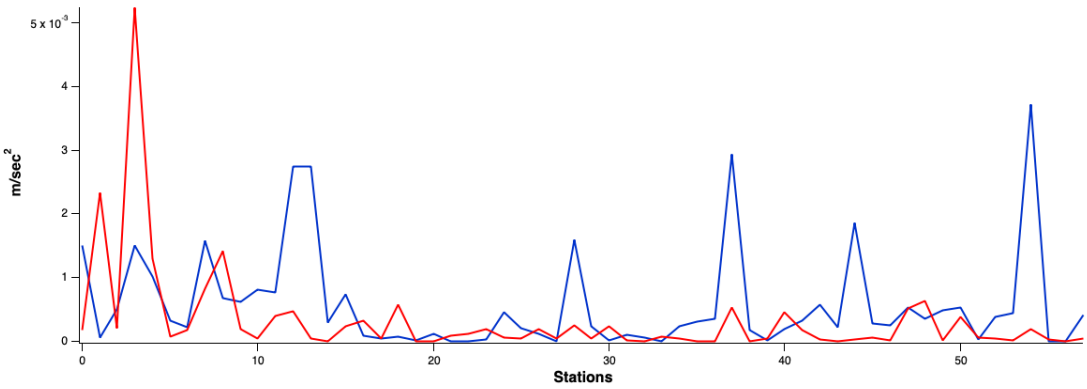

Figure 11. The inclinometer forward data (red) and return reversed data (blue)